

On the use of the equivalent source method for free-field calibration of an acoustic radiator in a reverberant tank

A.L. Virovlyansky¹ and M.S. Deryabin^{1,2}

¹Institute of Applied Physics, Russian Academy of Science, 46 Ul'yanov Street, Nizhny Novgorod, Russia,
viro@appl.sci-nnov.ru

²N.I. Lobachevsky State University of Nizhny Novgorod, 23 Prospekt Gagarina (Gagarin Avenue), Nizhny
Novgorod, Russia

Abstract

It is shown that the use of the equivalent source method allows one to reconstruct the sound field excited by an acoustic radiator in free space from the measurements of the sound field excited by this radiator in a tank with reflecting boundaries. The key assumption underlying the proposed approach is that the same set of monopoles with the same strengths can reproduce the field of the radiator both in free space and in the tank. The monopole strengths are reconstructed from the measurements in the tank, and the field in free space is then calculated using the known Green function. The feasibility of the approach is demonstrated in a tank experiment.

1 Introduction

Traditional approaches to solving the problem of free-field calibration of the acoustic radiator in a reverberant tank are based on the isolation of the direct signals arriving at the receivers without reflection from the tank boundaries. There are two conventional methods for eliminating the effect of boundary echoes [1, 2]. One of them is to coat the boundaries with absorbers. The second method relies on the time-gating technique for resolving the direct signals by their arrival times. However, both methods are applicable only at sufficiently high frequencies. There exist more sophisticated methods which can be used at acoustic frequencies below the limits imposed by the echo-free time of the test tank [3, 4].

In the present paper, we discuss an alternative approach that can be used for a free-field calibration of an acoustic radiator in a finite-sized tank without isolating the direct signal. To solve the problem, it is proposed to apply the well-known equivalent source method [5–10]. The sound field excited by the radiator is represented as a weighted superposition of fields excited by a set of acoustic monopoles called the equivalent sources. Our main assumption is that, under certain conditions set forth below, the radiator field in free space and in the tank can be reproduced by the same set of monopoles with the same strengths (amplitudes). The equivalent source strengths are reconstructed from the tank measurements. To solve this inverse problem, one needs to know the Green function of the Helmholtz equation in the tank. The required values of this function are obtained using the procedure that we call the tank calibration. It consists in placing the etalon monopole in the equivalent source positions and recording the emitted signals by all the receivers. The desired radiator field in free space is then readily evaluated using the reconstructed source strengths and the known Green function.

The paper is organized as follows. Section 2 outlines the main idea of our approach. The conditions under which it can be used are formulated and the procedure for solving the inverse problem is proposed. The tank experiment conducted to demonstrate the feasibility of this approach is described in Sec. 3. In section 4, it is shown, using the experimental data, that the same set of equivalent sources can reproduce the field of a single monopole both in free space and in a tank. Sec. 5 describes the reconstruction of the fields of acoustic dipole and quadrupole in free space from the measurement of their fields in the tank. The results of the paper are summarized in Sec. 6.

2 Equivalent source method

2.1 Free space

Consider a radiator exciting a monochromatic wave field at the carrier frequency f in free space with the sound speed c . In the framework of the equivalent source method, the complex field amplitude u at an arbitrary observation point \mathbf{r} is represented as a superposition of fields of acoustic monopoles located at N points $\mathbf{r}_1, \dots, \mathbf{r}_N$:

$$u(\mathbf{r}) = \sum_{n=1}^N G(\mathbf{r}, \mathbf{r}_n) A_n, \quad (1)$$

where

$$G(\mathbf{r}, \mathbf{r}_n) = \frac{1}{|\mathbf{r} - \mathbf{r}_n|} e^{ik|\mathbf{r} - \mathbf{r}_n|} \quad (2)$$

is the Green function in free space, $k = 2\pi f/c$ is the wave number, and A_n is the n -th source strength. Here, and in what follows, the time factor $e^{-2\pi i f t}$ is omitted.

To find the source strengths one should know the values of the field amplitude u at the collocation points $\boldsymbol{\rho}_1, \dots, \boldsymbol{\rho}_M$ covering the measurement surface S_M around the radiator (Fig. 1). The values of A_n should be found from the system of linear equations, in matrix form,

$$\mathbf{u} = \mathbf{G}\mathbf{A}, \quad (3)$$

where $\mathbf{u} = [u(\boldsymbol{\rho}_1), \dots, u(\boldsymbol{\rho}_M)]^T$ is the vector of field values measured at the collocation points, symbol T means transpose operation, \mathbf{G} is the matrix of size $M \times N$ with elements $G(\boldsymbol{\rho}_m, \mathbf{r}_n)$, $\mathbf{A} = [A_1, \dots, A_N]^T$ is the vector of unknown source strengths. In practice, the system of equations (3) is typically underdetermined "since there are often more waves in the model than measurement points" [11].

There are well-known methods for solving such systems of equations [11, 12]. One of them will be applied in this paper. It is based on the use of the singular value decomposition of matrix \mathbf{G} [13],

$$\mathbf{G} = \sum_{l=1}^L \gamma_l \boldsymbol{\xi}_l \boldsymbol{\eta}_l^H,$$

where γ_l are singular values numbered in descending order, $\boldsymbol{\xi}_l$ and $\boldsymbol{\eta}_l$ are singular vectors, and the symbol H denotes Hermitian conjugation. Neglecting the terms corresponding to small singular values, we obtain an estimate of the vector \mathbf{A}

$$\hat{\mathbf{A}} = \sum_{l=1}^{L_1} \frac{1}{\gamma_l} (\boldsymbol{\xi}_l^H \mathbf{u}) \boldsymbol{\eta}_l, \quad (4)$$

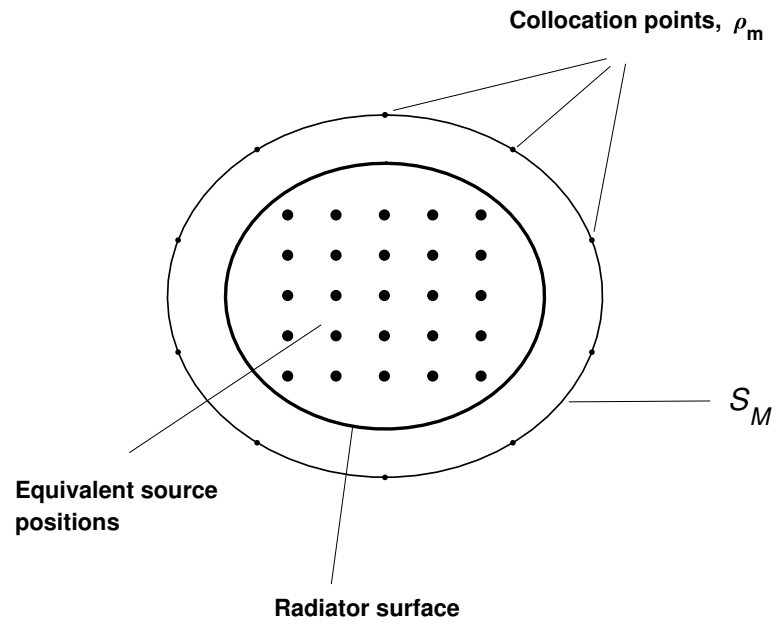


Figure 1: Sketch illustrating the equivalent source method. Equivalent source positions are located inside the area occupied by the radiator.

where $L_1 \leq L$ is the number of singular values taken into account. Substitution of this estimate into the right-hand side of Eq. (3) yields

$$\hat{\mathbf{u}} = \mathbf{G}\hat{\mathbf{A}} = \sum_{l=1}^{L_1} (\xi_l^H \mathbf{u}) \xi_l. \quad (5)$$

Parameter

$$\mu = \frac{\|\mathbf{u} - \hat{\mathbf{u}}\|}{\|\mathbf{u}\|}, \quad (6)$$

where the symbol $\|\dots\|$ denotes the Euclidean norm of the vector, quantitatively characterizes the accuracy with which the total field of equivalent sources approximates the radiated field at the collocation points. If the collocation points densely cover the measurement surface S_M and $\mu \ll 1$, then outside the area bounded by this surface, the equivalent sources well reproduce the field of the radiator.

A weak point of the equivalent source method is the lack of general rules for choosing the necessary number of equivalent sources and their positions [6, 10]. In practice, the problem of selecting the points \mathbf{r}_n and $\boldsymbol{\rho}_m$ is usually solved empirically, that is, through trial-and-error.

It should also be noted that due to the underdeterminedness of the system (3), its solution is ambiguous. Generally, there are many estimates $\hat{\mathbf{A}}$ (obtained using the relation (4) or found by other methods) that the vector $\hat{\mathbf{u}} = \mathbf{G}\hat{\mathbf{A}}$ approximates \mathbf{u} with high accuracy. It turns out that the estimates $\hat{\mathbf{A}}$, giving close $\hat{\mathbf{u}}$, may be quite different [11].

2.2 Tank

Consider a situation when the problem of approximating the radiator field in free space by a superposition of fields of acoustic monopoles is solved. It means that the positions \mathbf{r}_n of the equivalent sources and the source strengths A_n are chosen in such a way that the sum on the right-hand side of Eq. (1) with high accuracy approximates the radiator field outside some area σ_M . The latter can be a volume bounded by the measurement surface S_M , or a part of this volume.

Let us imagine that a reflecting boundary is placed in free space outside the area σ_M . The radiator and the equivalent sources excite practically equal waves incident on this boundary. It is clear that after reflection from the same boundary, the waves will remain equal. Moreover, if the radiator is sufficiently small, its field and the total field of equivalent sources will remain approximately the same, even in the presence of several boundaries, when the waves experience multiple reflections. The smallness of the radiator is required because the waves reflected from the boundaries 'do not notice' the monopole equivalent sources, but they are

scattered on the radiator of finite size. It is natural to expect that with a sufficiently small radiator size, the effect of this scattering will be insignificant.

Based on the above elementary reasoning, we will assume that a set of equivalent sources simulating the fields of a radiator in free space can be used to represent the field of this radiator in a tank with reflecting boundaries. In both cases, the sources are located within the same area σ_M . In the tank, Eq. (1) translates to

$$\tilde{u}(\mathbf{r}) = \sum_{n=1}^N \tilde{G}(\mathbf{r}, \mathbf{r}_n) A_n, \quad (7)$$

where $\tilde{G}(\mathbf{r}, \mathbf{r}_n)$ is the field of the acoustic monopole (Green function) in the tank, \mathbf{r}_n and A_n are, respectively, **the same** positions and strengths of the equivalent sources as in Eq. (1). We assume that this representation of the radiator field in the tank is valid under the following conditions.

- (i) The sound speed in the tank is constant and equal to its value in free space.
- (ii) The area σ_M can fit entirely in the tank. Equation (7) describes the sound field only at points \mathbf{r} located outside σ_M .
- (iii) The radiator in the tank works in the same way as in free space: each point of its surface in both cases oscillates according to the same law.
- (iv) The radiator sizes are small compared to the tank sizes.

Our idea of restoring the radiator field in free space from the measurements in a tank is based on the conjecture that the opposite is also true. We suppose that if a set of equivalent sources reproduces the radiator field in the tank, then the field of the same radiator in free space is well approximated by the same set of equivalent sources, that is, by the monopoles with the same \mathbf{r}_n and A_n . As in free space, the field in the tank should be measured at the collocation points $\boldsymbol{\rho}_1, \dots, \boldsymbol{\rho}_M$. Field amplitudes at these points form the vector $\tilde{\mathbf{u}} = [\tilde{u}(\boldsymbol{\rho}_1), \dots, \tilde{u}(\boldsymbol{\rho}_M)]^T$. From Eq. (7) we find a system of linear equation similar to (3):

$$\tilde{\mathbf{u}} = \tilde{\mathbf{G}}\mathbf{A}, \quad (8)$$

where $\tilde{\mathbf{G}}$ is a matrix of size $M \times N$ with the elements $\tilde{G}(\boldsymbol{\rho}_m, \mathbf{r}_n)$, \mathbf{A} is a vector of the source strengths. In contrast to the free space, the Green function $\tilde{G}(\boldsymbol{\rho}, \mathbf{r})$ in the tank is unknown. Therefore, the quantities of $\tilde{G}(\boldsymbol{\rho}_m, \mathbf{r}_n)$ for each pair $(\boldsymbol{\rho}_m, \mathbf{r}_n)$ must be measured. To this end, one should use a reference acoustic monopole, alternately placed at each of the points \mathbf{r}_n . The complex amplitude of the tone emitted from the point \mathbf{r}_n and received at the point $\boldsymbol{\rho}_m$ is proportional to $\tilde{G}(\boldsymbol{\rho}_m, \mathbf{r}_n)$. The procedure of measuring the coefficients $\tilde{G}(\boldsymbol{\rho}_m, \mathbf{r}_n)$ we call the tank calibration.

The desired radiator field in free space is calculated by the formula (1) after substituting into it the source strengths A_n , found from the solution of system (8).

3 Tank experiment

To test the feasibility of the proposed approach, as well as the validity of the assumptions underlying it, a tank experiment was conducted. For its implementation was used the experimental setup developed on the basis of a measurement system (Ultrasound Measurement System Control Centre produced by Precision Acoustics company) which includes an organic-glass container of dimensions 1x1x1 m (Fig. 2) [14]. This container played the role of our tank. It was filled with clean degassed and deionized water with a specific resistance of at least 18 MOhm*cm, which was produced by a DM-4B membrane-type distiller unit. The water temperature was monitored with a thermometer and was measured at $24 \pm 0.1^\circ\text{C}$ in the experiment.

Two reversible hydrophones B & K8103 were used to tank calibration. Each of them has an operating band of up to 180 kHz, with dimensions of 10×16 mm. Both hydrophones were attached to the manipulators through metal tubes 10 mm in diameter with the length of the submerged part up to 0.5 m. The absolute accuracy of the manipulator-assisted motion amounts to $6 \mu\text{m}$.

The positions of the hydrophones in the tank will be described using the Cartesian coordinate system (x, y, z) with the y axis directed vertically upwards.

One of the hydrophones was used as a sound source. The radiation was carried out at the carrier frequency $f = 13.7$ kHz, which corresponds to the wavelength $\lambda = 10.8$ cm. Since the hydrophone dimensions indicated above are small compared to λ , this sound source was an acoustic monopole. It was alternately placed into points \mathbf{r}_n forming a $7 \times 7 \times 7$ cube, whose center coincided with the origin. Figure 3 shows the cross section of this cube in the $x = 0$ plane. The distance between the nearest points of the cube is 1 cm, that is, about 0.1λ .

The second hydrophone was used as a sound receiver. It was located in five positions $\boldsymbol{\rho}_1, \dots, \boldsymbol{\rho}_5$, shown in Fig. 3 by bold dots. The step size between the neighboring receiver positions is 5 cm. They are placed along a straight line parallel to the y axis. The line is shifted at the distance $h = 38.5$ cm from the origin.

The measurements were performed as follows. While the receiving hydrophone was located at one the points $\boldsymbol{\rho}_1, \dots, \boldsymbol{\rho}_5$, the hydrophone playing the role of the source was placed in turn at all $7^3 = 343$ points \mathbf{r}_n forming the cube. From each point it emitted the same tonal



Figure 2: Experimental setup.

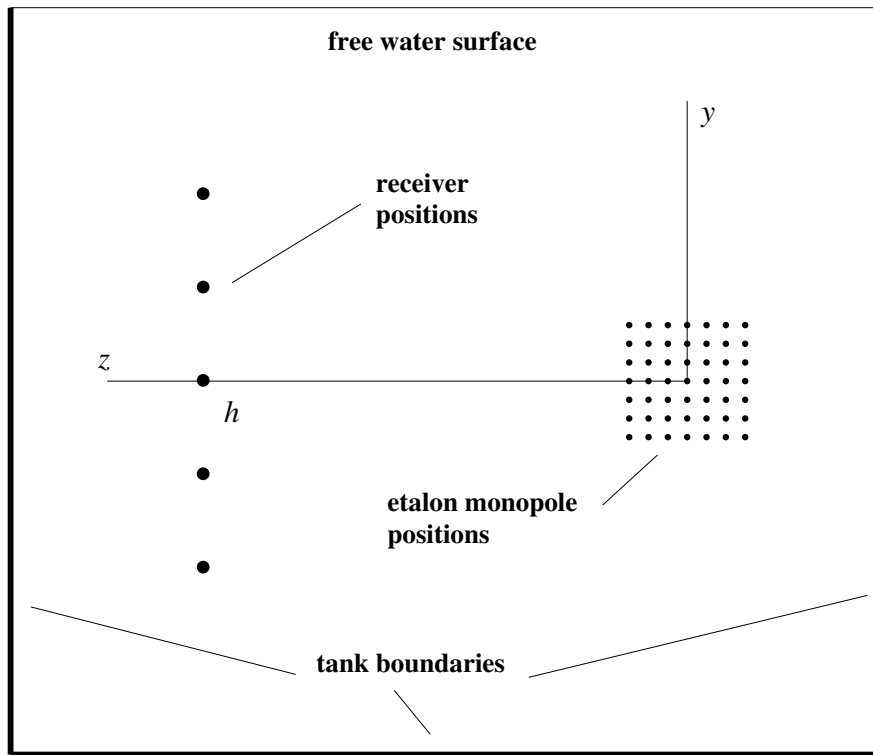


Figure 3: Section of the tank in the plane $x = 0$. Location of the receiver positions and points at which the etalon monopole was placed during the tank calibration.

signal at frequency f , which was recorded by the receiver. Registration began with a delay of $\tau = 2000$ ms after the start of radiation. During the time τ , all the transients associated with the reflections from the boundaries and resonant behavior of the source ended and the received signal was an almost perfect sinusoid. The signal emitted from the point \mathbf{r}_n and recorded at the point $\boldsymbol{\rho}_m$ was a piece of sinusoid $g_{m,n} \sin(2\pi ft - \phi_{m,n})$ including of about 27 periods of the carrier frequency. The time t for each signal was reckoned from the start of the radiation $t = 0$. The complex demodulate of this signal $g_{m,n} \exp(i\phi_{\mu,n})$ is equal to $C\tilde{G}(\boldsymbol{\rho}_m, \mathbf{r}_n)$, where C is some constant complex factor that is the same for all pairs (m, n) . In what follows, we will compare only linear combinations of $\tilde{G}(\boldsymbol{\rho}_m, \mathbf{r}_n)$ among themselves and, therefore, the factor C will be omitted.

In the course of the experiment, $5 \times 343 = 1715$ complex values of the Green's function in the tank, $\tilde{G}(\boldsymbol{\rho}_m, \mathbf{r}_n)$, were measured. These data were used to test the approach under consideration. The results are presented in the next sections.

4 Approximation of the acoustic monopole field using 6 and 8 equivalent sources

We begin by checking the assumption that under conditions (i) - (iv) listed in Sec. 2.2 the same set of equivalent sources (acoustic monopoles) reproducing the field of a given radiator in free space reproduces the field of this radiator in the tank. To this end, consider two simple examples in which the source strengths A_n in Eq. (1) are found analytically.

In both examples, the role of the radiator is played by an acoustic monopole located at the point $\mathbf{r} = 0$ and exciting the field $G(\mathbf{r}, 0) = \exp(ikr)/r$, where $r = |\mathbf{r}|$. Further, this monopole will be called central. The function $G(\mathbf{r}, 0)$ will be approximated by a superposition of fields of equivalent sources representing exactly the same monopoles.

In the first example, we consider 6 equivalent sources located at the points $\mathbf{q}_{1,2} = (\pm a, 0, 0)$, $\mathbf{q}_{3,4} = (0, \pm a, 0)$, $\mathbf{q}_{5,6} = (0, 0, \pm a)$, that is, shifted relative to the central monopole at distances of $\pm a$ along each of the coordinate axes (Fig. 4a). Let us show that under the condition

$$ka < 1 \tag{9}$$

the equivalent source strengths can be chosen in such a way that in the far field, that is, at $r \gg a^2/\lambda$, they approximate the central monopole field $G(\mathbf{r}, 0)$ with good accuracy. From symmetry considerations, it is clear that all the source strengths should be equal to the same value, which we denote by B_6 . It should be found from the condition that in the far zone

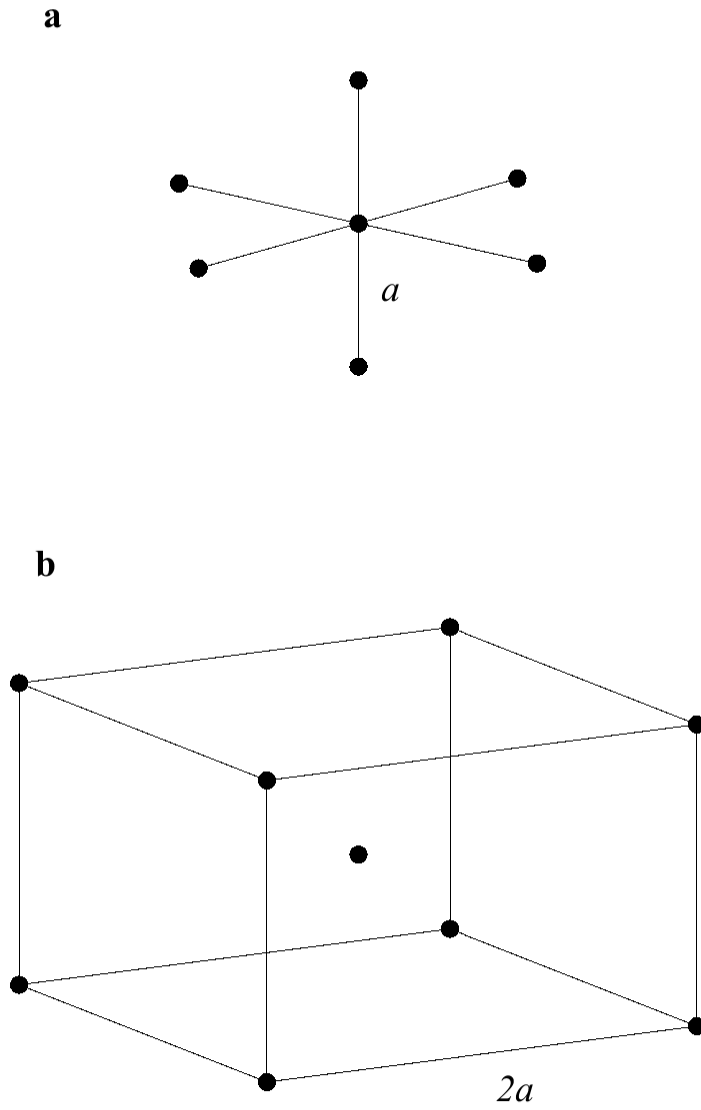


Figure 4: The central monopole surrounded by 6 (a) and 8 (b) monopoles, considered as equivalent sources.

the equality

$$G(\mathbf{r}, 0) = B_6 \sum_{n=1}^6 G(\mathbf{r}, \mathbf{q}_n) \quad (10)$$

holds. In the far zone

$$\begin{aligned} \sum_{n=1}^6 G(\mathbf{r}, \mathbf{q}_n) &= \frac{e^{ikr}}{r} \sum_{n=1}^6 e^{-ik\boldsymbol{\nu}\mathbf{q}_n} \\ &= 2\frac{e^{ikr}}{r} [\cos(ka\nu_x) + \cos(ka\nu_y) + \cos(ka\nu_z)], \end{aligned} \quad (11)$$

where $\boldsymbol{\nu} = \mathbf{r}/r$ is the unit vector whose projections onto the axes of the Cartesian coordinate system (x, y, z) we denote ν_x , ν_y , and ν_z , respectively. When the condition (9) is met, the cosine arguments in the last expression are relatively small and we can use the approximation

$$\cos \alpha \simeq 1 - \alpha^2/2. \quad (12)$$

Since $\nu_x^2 + \nu_y^2 + \nu_z^2 = 1$, we find

$$\sum_{n=1}^6 G(\mathbf{r}, \mathbf{q}_n) = \frac{e^{ikr}}{r} [6 - (ka)^2].$$

It follows that the equality (10) holds when

$$B_6 = \frac{1}{6} + \frac{(ka)^2}{36}. \quad (13)$$

Our assumption is that Eq. (10) in the tank translates to

$$\tilde{G}(\mathbf{r}, 0) = B_6 \sum_{n=1}^6 \tilde{G}(\mathbf{r}, \mathbf{q}_n), \quad (14)$$

where B_6 is the same coefficient defined by Eq. (13) as in free space, but the Green function $\tilde{G}(\mathbf{r}, \mathbf{q}_n)$, which accounts for multiple reflections from the boundaries, is quite different from $G(\mathbf{r}, \mathbf{q}_n)$.

To verify this statement, we use the quantities $\tilde{\mathbf{G}}(\boldsymbol{\rho}_m, \mathbf{r}_n)$ measured in the tank experiment described in the previous section. As the position of the central monopole \mathbf{r}_* , take one of the points r_n that does not lie on the boundary of the cube. In this case, the roles of $\mathbf{q}_1, \dots, \mathbf{q}_6$ will play cube points shifted relative to \mathbf{r}_* along each of the coordinate axes by $\pm a$, where $a = 1$ cm. So we have $ka = 0.58$ which satisfies the condition (9). Substituting this value into Eq. (13) yields

$$B_6 = 0.176. \quad (15)$$

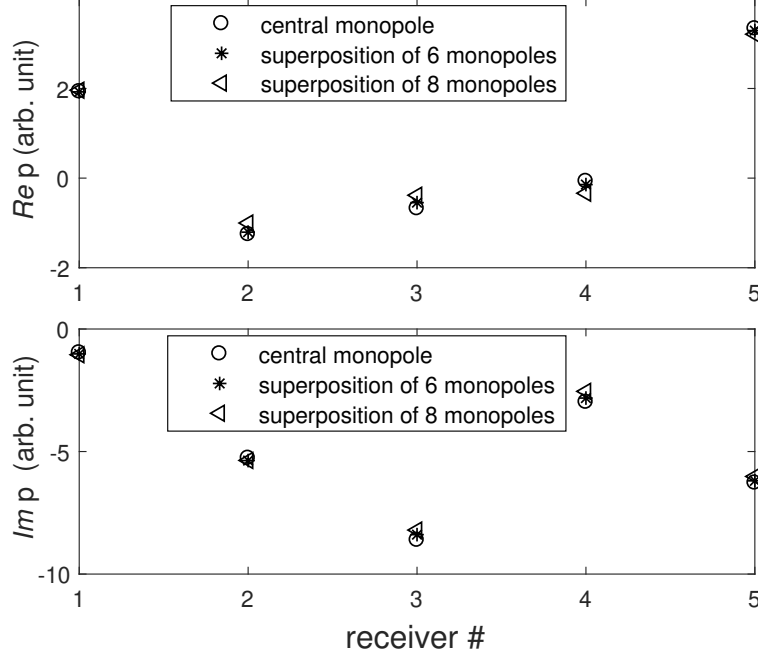


Figure 5: Real (top) and imaginary (bottom) parts of pressure amplitudes at receiving points. Circles: signal of the central monopole. Asterisks: the sum of signals from 6 monopoles with weight B_6 . Triangles: the sum of signals from 8 monopoles with weight B_8 .

Although our value of ka is not very small, the difference between the left and right sides of Eq. (10) with this value of B_6 at distances from the central monopole exceeding 5 cm is less than 0.5 %. Therefore, a ball with a radius of 5 cm, centered at \mathbf{r}_* , can be considered as the area σ_M introduced in Sec. 2.2. The points $\mathbf{p}_1, \dots, \mathbf{p}_5$ lie outside this ball.

In Fig. 5, circles show the real (top) and imaginary (bottom) parts of the complex pressure amplitudes p (in arbitrary units) recorded at all five receiver positions after the etalon monopole has been placed at \mathbf{r}_* . Asterisks show the real and imaginary parts of the pressures obtained by summing the fields of the etalon monopole emitted from the six points closest to \mathbf{r}_* with the weighting factor (15). In other words, the asterisks present the field amplitude values calculated by the formula (14). Similar results are obtained with other choices of the central monopole position \mathbf{r}_* (not shown). Thus, experimental data confirm the applicability of Eq. (14).

As a second example, consider the approximation of the acoustic monopole field by the fields of eight equivalent sources located at the points $\mathbf{p}_{1,\dots,8} = (\pm a, \pm a, \pm a)$, that is, at the

vertices of a cube with an edge of length $2a$ (Fig. 4b). The monopole playing the role of a radiator is located in the center of this cube. As in the previous example, the strengths of all the equivalent sources should be the same. In this example, Eq. (10) turns to

$$G(\mathbf{r}, 0) = B_8 \sum_{m=1}^8 G(\mathbf{r}, \mathbf{p}_m). \quad (16)$$

In the far zone

$$\begin{aligned} \sum_{m=1}^8 G(\mathbf{r}, \mathbf{p}_m) &= \frac{e^{ikr}}{r} \sum_{m=1}^8 e^{-ik\mathbf{n}\mathbf{p}_m} \\ &= 2\frac{e^{ikr}}{r} [\cos(ka(n_x + n_y + n_z)) + \cos(ka(-n_x + n_y + n_z)) \\ &\quad + \cos(ka(n_x - n_y + n_z)) + \cos(ka(-n_x - n_y + n_z))]. \end{aligned}$$

Assuming that the condition (9) is fulfilled and again using the approximation (12), we find

$$\sum_{m=1}^8 G(\mathbf{r}, \mathbf{p}_m) = \frac{e^{ikr}}{r} [8 - 4(ka)^2]. \quad (17)$$

The equality (16) holds when

$$B_8 = \frac{1}{8} + \frac{(ka)^2}{16}. \quad (18)$$

In the tank, the analogue of Eq. (16) has the form (cf. Eq. (14))

$$\tilde{G}(\mathbf{r}, 0) = B_8 \sum_{n=1}^8 \tilde{G}(\mathbf{r}, \mathbf{p}_n). \quad (19)$$

Substituting $ka = 0.58$ in Eq. (18) yields

$$B_8 = 0.149. \quad (20)$$

As σ_M we can take the same ball as in the previous example. Outside this ball in free space, the difference between the left and right sides of Eq. (16) does not exceed 3%.

To test Eq. (19), we again use our experimental data. The triangles in Fig. 5 present the result of summing the fields emitted from 8 points located at the vertices of the cube shown in Fig. 4b. Fields are summed with the weight factor (20). The cube center is the same point \mathbf{r}_* , which was considered in the previous example. Similar results were obtained for other points of the cube selected as \mathbf{r}_* (not shown).

5 Reconstruction of sound fields excited by a dipole and quadrupole

Let us use the data of our measurements to verify the method of restoring the radiator field in free space, formulated in Sec. 2.2. In the central part of the cube of size $7 \times 7 \times 7$ formed by the points in which the etalon monopole was placed, we select a small cube of size $3 \times 3 \times 3$ so that both cubes are centered at point $\mathbf{r} = 0$. The points of the big cube that are not included in the small one will be considered as positions of the equivalent sources and denoted by the symbols $\tilde{\mathbf{r}}_n$, $n = 1, \dots, 316$.

We will use the superpositions of signals emitted from the points of a small cube to simulate the fields of the dipole and quadrupole sound sources. Take two points of a small cube, which lie on the y -axis and in Fig. 6 are marked with $+$ and $-$. Denote their positions as \mathbf{r}_+ and \mathbf{r}_- . The difference of the fields emitted by the etalon monopole from these points, that is, $\tilde{u}(\mathbf{r}) = \tilde{G}(\mathbf{r}, \mathbf{r}_+) - \tilde{G}(\mathbf{r}, \mathbf{r}_-)$, represents the field of the acoustic dipole in the tank. In the process of tank calibration, the values of $\tilde{G}(\boldsymbol{\rho}_m, \mathbf{r}_\pm)$, $m = 1, \dots, 5$, were measured. This allows us to find the complex amplitudes of the dipole field at the reception points $\tilde{\mathbf{u}} = [\tilde{u}(\boldsymbol{\rho}_1), \dots, \tilde{u}(\boldsymbol{\rho}_5)]^T$. This vector represents the right-hand side of the system (8), which is to be solved for unknown source strengths A_n . The elements of matrix $\tilde{\mathbf{G}}$ were actually measured during the tank calibration.

Thus, we obtained a strongly underdetermined system: there are only 5 equations for finding 316 unknown A_n . Besides, intuition suggests that in order to reconstruct the radiator field, receivers should surround it on all sides.

Fortunately, the underdeterminedness of the problem can be significantly reduced without additional measurements. Consider the rotations of our dipole by 90° , 180° , and 270° about each of the x , y and z axes. Since at each rotation the points \mathbf{r}_+ and \mathbf{r}_- fall into other points of the small cube, for each of the ten resulting dipole positions (original position and 9 rotations) we can easily find the corresponding vector of field amplitudes on the receivers $\tilde{\mathbf{u}} = \tilde{\mathbf{u}}_j$, $j = 1, \dots, 10$.

Note that the rotation of the dipole allows us to get by with a smaller number of receivers. Instead of using receivers surrounding the dipole from all sides, we alternately turn its different sides to the 5 existing receivers.

In accordance with our assumptions, formulated in Sec. 2.2, the dipole at any turn is associated with the same equivalent sources that should be rotated with it. For each of the turns described above, the equivalent sources only change places: the equivalent source from the point $\tilde{\mathbf{r}}_n$ falls into the point $\tilde{\mathbf{r}}_m$, representing the position of another equivalent source.

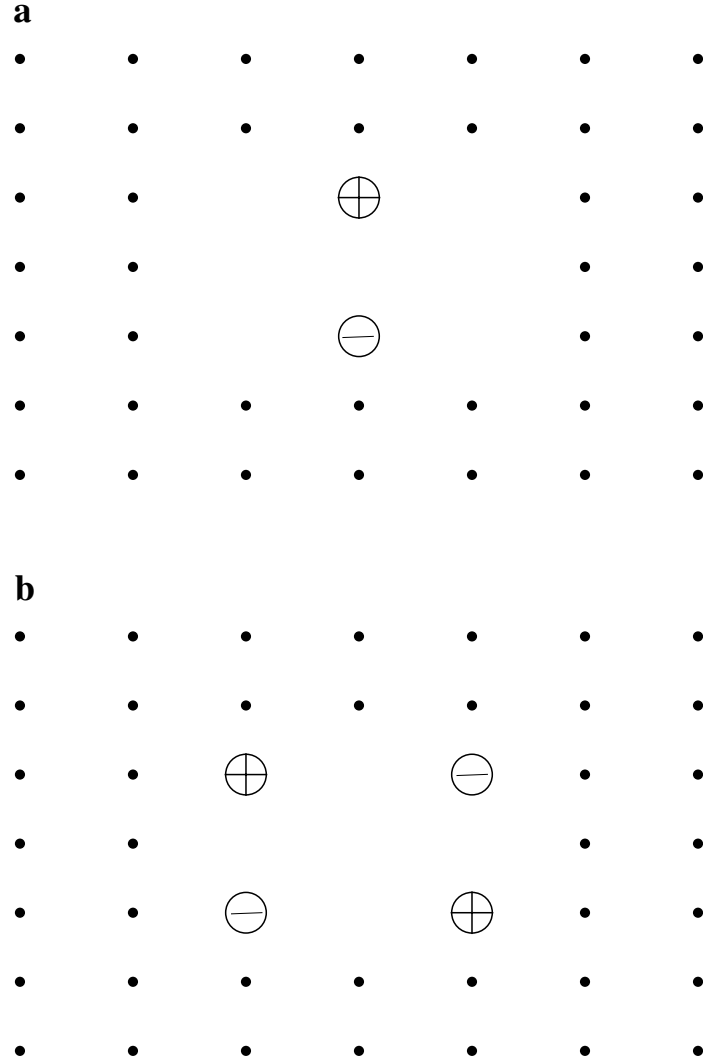


Figure 6: Dipole (a) and quadrupole (b) sources. Points indicate the equivalent source positions. Circles represent the monopole sources placed at the points of the small cube. Symbols $+$ and $-$ indicate the signs of the monopole source strengths.

Then, the source strength at the point $\tilde{\mathbf{r}}_m$ becomes equal to A_n . This means that the rotation of the dipole results in a permutation of the elements of the vector \mathbf{A} . For the j -th dipole position, the system of equations (3) takes the form

$$\tilde{\mathbf{u}}_j = \tilde{\mathbf{G}}\mathbf{T}_j\mathbf{A}, \quad (21)$$

where \mathbf{T}_j is a permutation matrix of size 316×316 , describing the permutation of the elements of vector \mathbf{A} caused by the rotation.

Combining 10 vectors $\tilde{\mathbf{u}}_j$ into one vector and 10 matrices $\tilde{\mathbf{G}}\mathbf{T}_j$ into one matrix,

$$\tilde{\mathbf{u}}_c = \begin{pmatrix} \tilde{\mathbf{u}}_1 \\ \vdots \\ \tilde{\mathbf{u}}_{10} \end{pmatrix}, \quad \tilde{\mathbf{G}}_c = \begin{pmatrix} \tilde{\mathbf{G}}\mathbf{T}_1 \\ \vdots \\ \tilde{\mathbf{G}}\mathbf{T}_{10} \end{pmatrix},$$

we get a system of 50 equations for 316 unknowns A_n :

$$\tilde{\mathbf{u}}_c = \tilde{\mathbf{G}}_c\mathbf{A}. \quad (22)$$

So, the rotations of the dipole and equivalent sources at the angles indicated above allowed us to increase the number of equations by a factor of 10 without increasing the number of receivers and without additional measurements.

It should be noted that there are 24 different rotations of the cube, in which its points exchange places: the lower side of the cube can be selected in 6 ways and this side can then be rotated into 4 different positions. We use only 10 rotations since this is sufficient to reconstruct the fields of the simplest sources considered in this paper.

To solve the system (22), we use the method described in Sec. 2.1. The desired estimate of the vector \mathbf{A} is given by the formula (4), in which γ_l are the singular numbers of the matrix $\tilde{\mathbf{G}}_c$ (see Fig. 7), $\boldsymbol{\xi}_l$ and $\boldsymbol{\eta}_l$ are the singular vectors. For each value of L_1 from 1 to 50, Eq. (4) gives an approximate solution of the system (22). A quantitative estimate of the accuracy of each solution is given by the parameter μ determined by Eq. (6) with $\mathbf{u} = \tilde{\mathbf{u}}$ and $\hat{\mathbf{u}} = \tilde{\mathbf{G}}_c\hat{\mathbf{A}}$. The dependence of μ on L_1 is shown in the upper panel of Fig. 8.

Substituting the found source strengths A_n into Eq. (1) gives an approximate expression for the field excited by the dipole source in free space $u(\mathbf{r})$. To estimate the reconstruction accuracy, we compare the values of the function found $u(\mathbf{r})$ on a spherical surface of radius $R = 1$ m in free space with the values on the same surface of the function $u_e(\mathbf{r}) = G(\mathbf{r}, \mathbf{r}_+) - G(\mathbf{r}, \mathbf{r}_+)$ representing the exact expression of the field excited by our dipole. The points of this surface are given by the relations $x = R \cos \varphi \sin \theta$, $y = R \sin \phi \sin \theta$, $z = R \cos \theta$, where ϕ and θ are azimuthal and polar angles, respectively. Choosing discrete angles ϕ_m ,

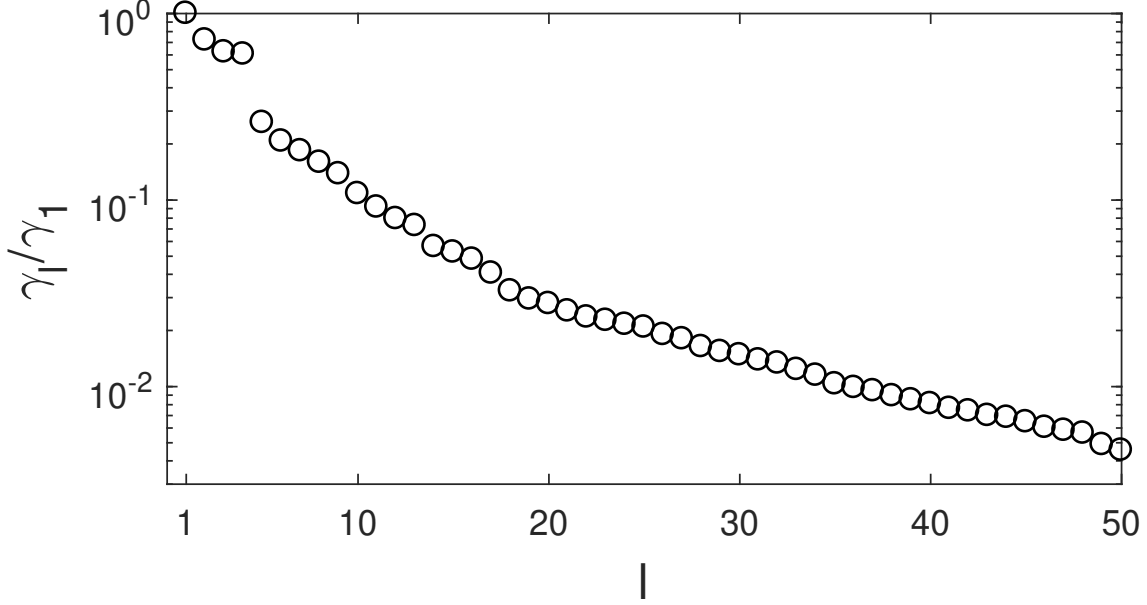


Figure 7: Singular values of matrix $\tilde{\mathbf{G}}_c$ divided by the greatest of them.

$m = 1, \dots, 100$, and θ_n , $n = 1, \dots, 90$ uniformly sampling the intervals $0 \leq \phi \leq 2\pi$, and $0 \leq \theta \leq \pi$, respectively, we get sampling points \mathbf{r}_{mn} on the selected surface. By analogy with (6) as a quantitative measure of the proximity of the $u(\mathbf{r})$ and $u_e(\mathbf{r})$ we take

$$\mu_R = \left(\frac{\sum_{m,n} |u(r_{mn}) - u_e(r_{mn})|^2}{\sum_{m,n} |u_e(r_{mn})|^2} \right)^{1/2}, \quad (23)$$

where the summation goes over all sampling points. The lower panel in Fig. 8 shows the values of μ_R for all possible values of L_1 . As we see, for all $L_1 \geq 4$ both μ and μ_R are small compared to the unity. This means that with such L_1 , the inverse problem is solved with satisfactory accuracy.

Figure 9 shows the amplitudes $|u_e(\mathbf{r})|$ (upper panel) and $|u(\mathbf{r})|$ (lower panel) on the spherical surface as functions of the azimuthal and polar angles. These plots actually represent the exact and reconstructed directivity patterns of the dipole source. Amplitude $|u(\mathbf{r})|$, whose distribution on the spherical surface is shown in the lower panel, is calculated with $L_1 = 8$. The distributions of amplitudes $|u(\mathbf{r})|$ for all L_1 from interval $4 \leq L_1 \leq 50$ look likewise.

It is worth noting, that despite the proximity of the functions $u(\mathbf{r})$ found for all L_1 from the above interval, the source strengths corresponding to different L_1 are generally strongly

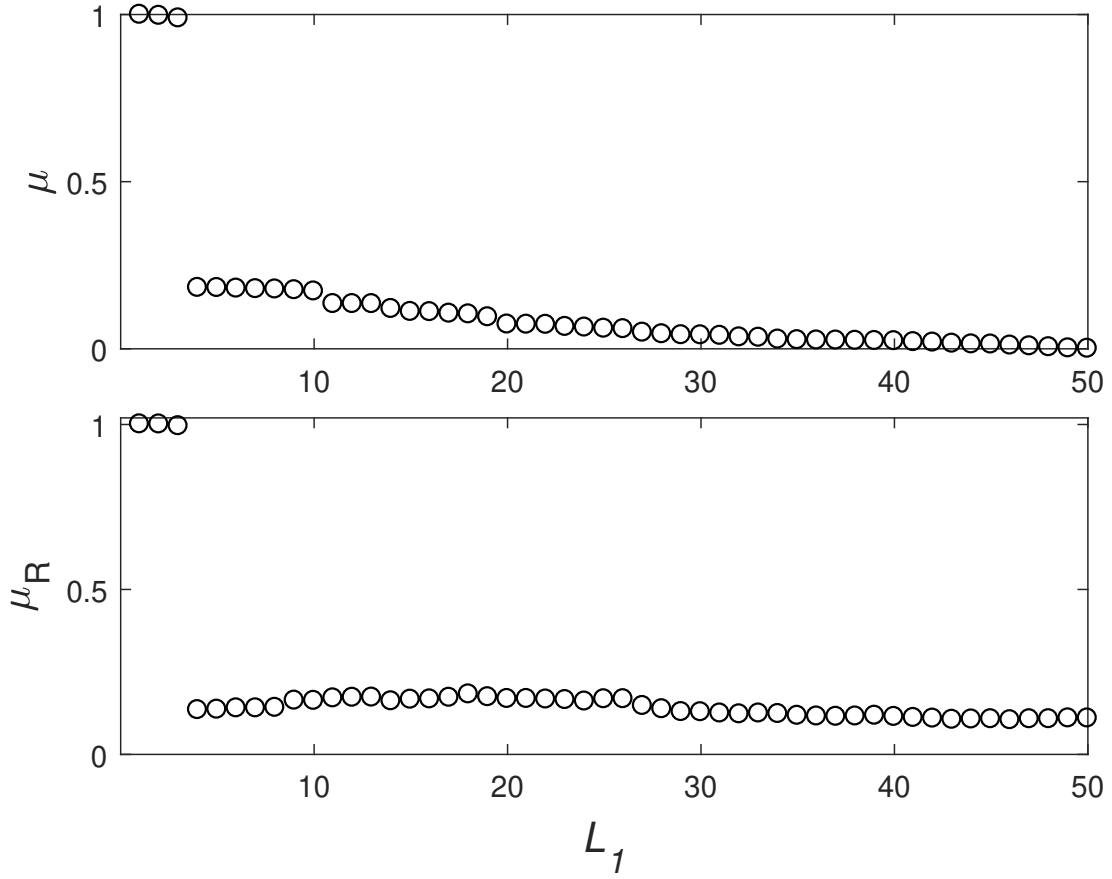


Figure 8: Upper panel: parameter μ quantitatively characterizing the closeness of the measured and reconstructed field at the collocation points as a function of L_1 , the number of singular values taken into account. Lower panel: similar dependence for parameter μ_R quantitatively characterizing the accuracy of the reconstructed dipole field in free space.

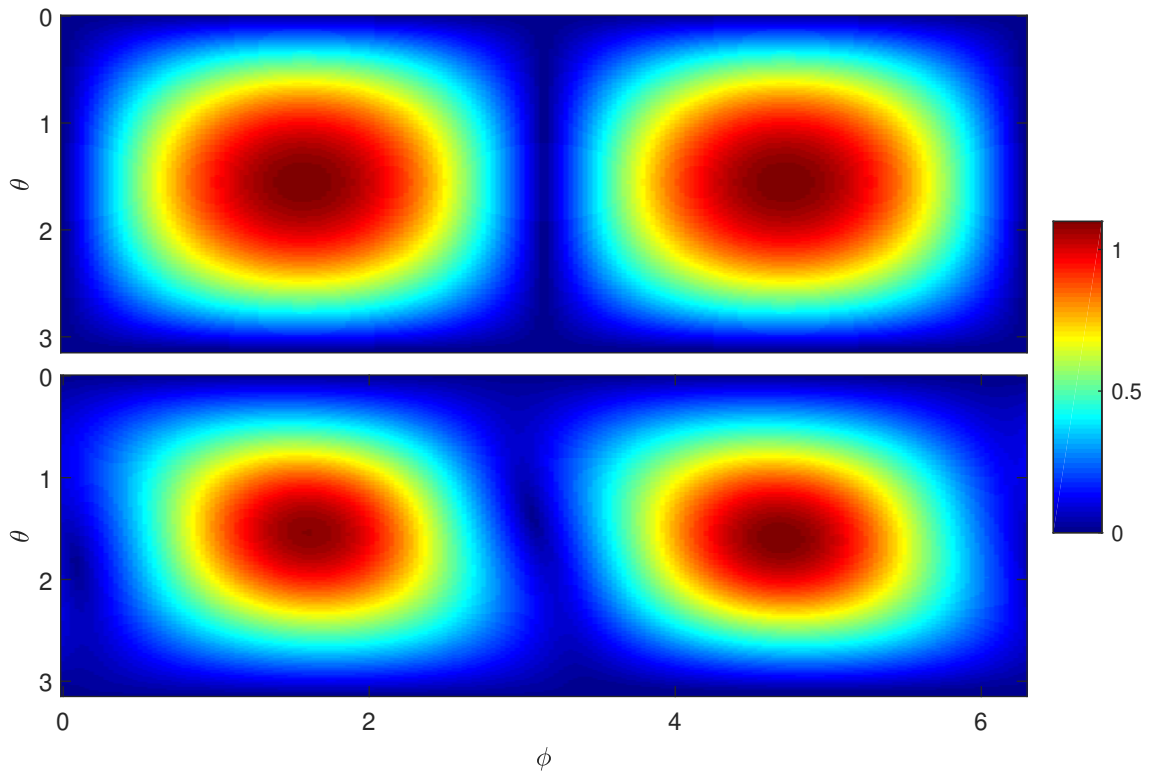


Figure 9: Field amplitude at 1 m from the dipole center in free space as a function of azimuth angle ϕ and polar angle θ . Upper panel: exact analytic solution. Lower panel: result of the reconstruction with $L_1 = 8$.

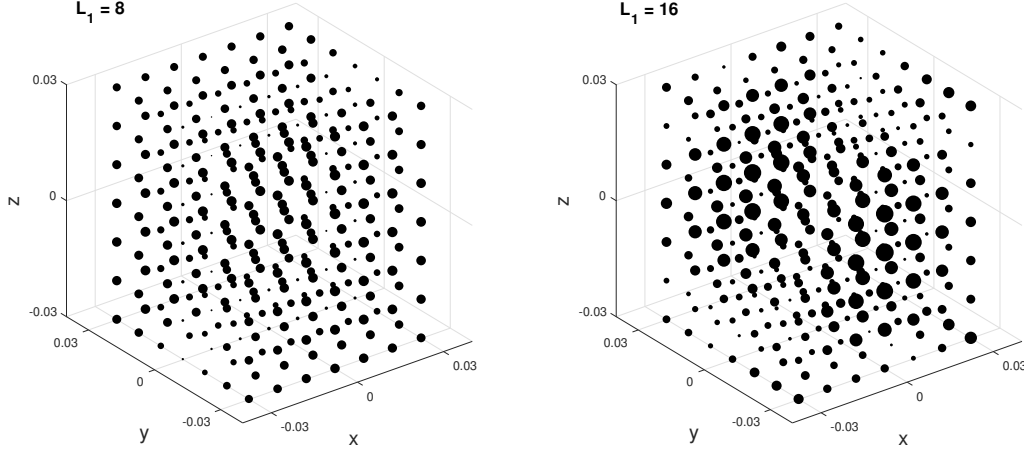


Figure 10: Equivalent source strengths found by solving the system (22) with the account of 8 (left panel) and 16 (right panel) singular values and vectors.

different. To illustrate this statement, Fig. 10 shows the absolute values of source strength found with $L_1 = 8$ (left panel) and $L_1 = 16$ (right panel). The size of a point whose center is located at the position of the n -th equivalent source is proportional to $|A_n|$.

Similarly, it is possible to reconstruct the field of a quadrupole in free space. Its field in the tank can be synthesized from the fields emitted by the etalon monopole from four points of the small cube shown in Fig. 6b. In this example, the four points are located in the $x - y$ plane. The inverse problem again reduces to solving the system (22) with the same matrix $\tilde{\mathbf{G}}_c$ but different $\tilde{\mathbf{u}}_c$. As in the case of dipole, the source strengths A_n , found by the formula (4), are to be substituted in Eq. (1). To estimate the accuracy of the reconstruction, the same parameters μ and μ_R are used as for the dipole. Figure 11 presents the dependencies of these parameters on L_1 , the number of singular values and vectors taken into account. As we see, for the quadrupole these parameters are small for $L_1 \geq 8$. Figure 12 shows the amplitude distributions of the quadrupole field on the spherical surface of radius $R = 1$ cm calculated using the exact analytical formula (upper panel) and reconstructed by solving the inverse problem with $L_1 = 8$ (lower panel). As in the case of the dipole, these directivity patterns coincide well. The same is true for all L_1 from interval $8 \leq L_1 \leq 50$ (not shown).

Similar results were obtained when reconstructing the field of a quadrupole located in the $x - z$ plane. Exact and reconstructed (with $L_1 = 8$) directivity patterns of this quadrupole are presented in Fig. 13.

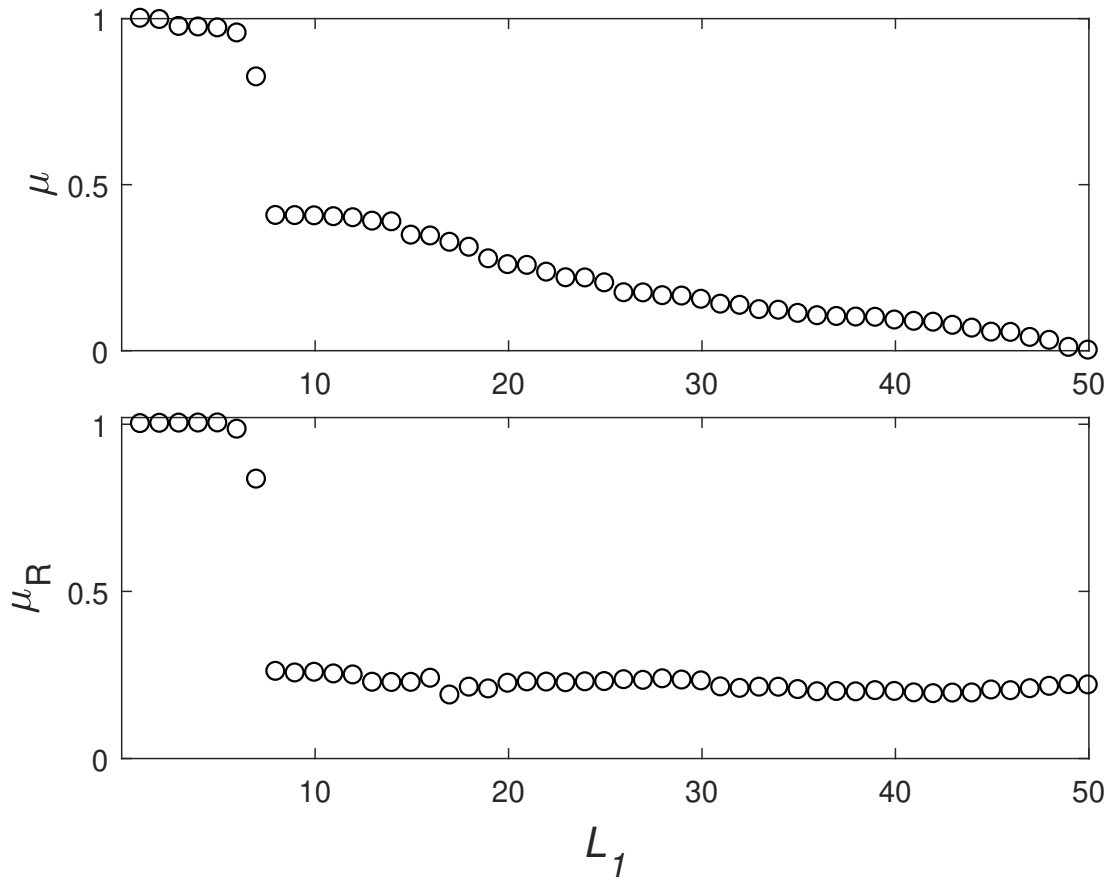


Figure 11: The same as in Fig. 8, but for the quadrupole in the plane $x - y$.

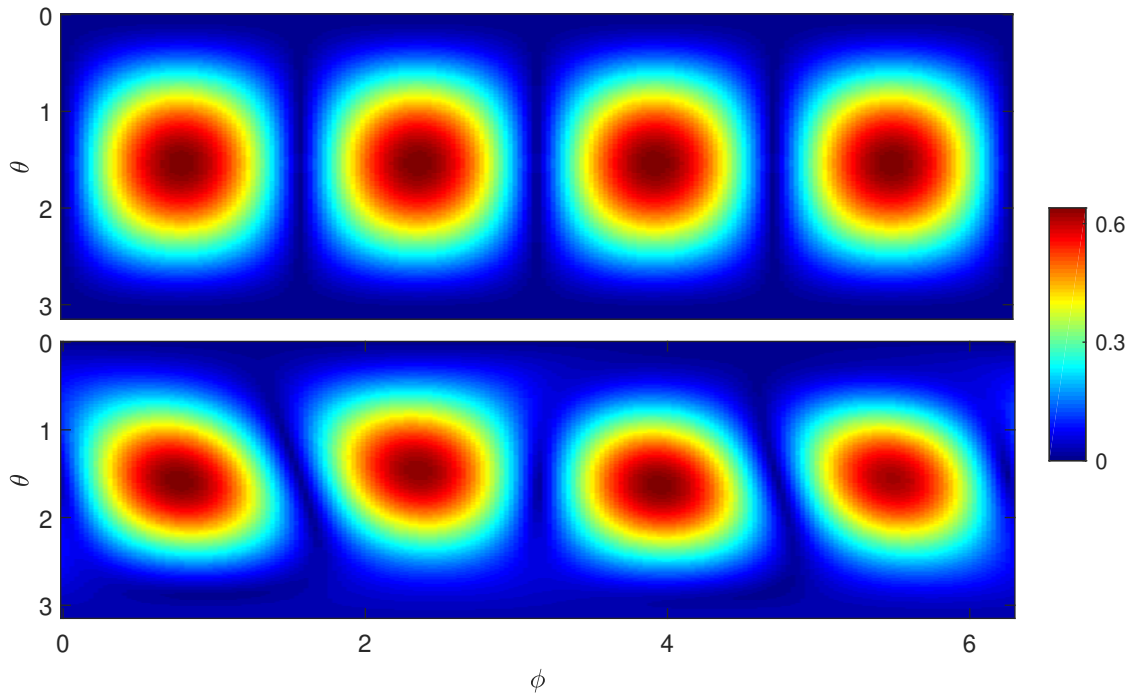


Figure 12: The same as in Fig. 9, but for the quadrupole in the plane $x - y$. Upper panel: exact analytic solution. Lower panel: result of the reconstruction with $L_1 = 8$.

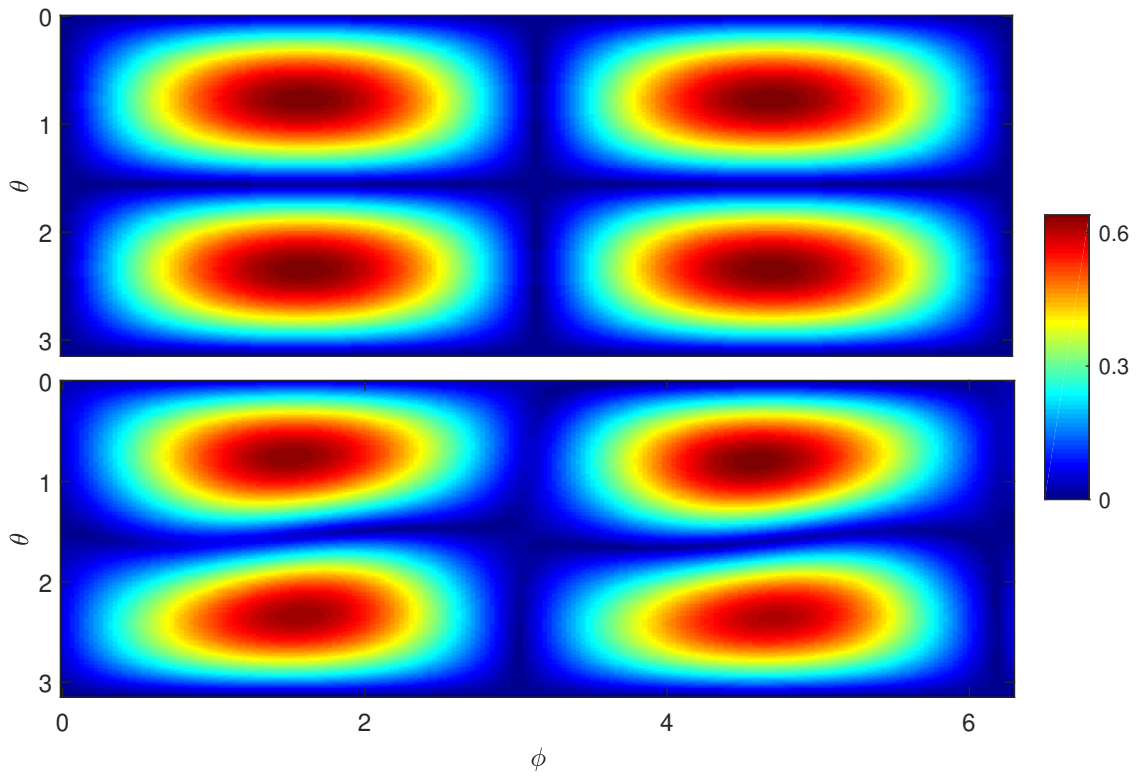


Figure 13: The same as in Fig. 9, but for the quadrupole in the plane $x - z$. Upper panel: exact analytic solution. Lower panel: result of the reconstruction with $L_1 = 8$.

We also considered the field excited by a monopole located at one of the points of the small cube (not shown). Its field in free space is successfully reconstructed with $L_1 \geq 2$.

6 Conclusion

The paper shows that the use of the equivalent source method makes it possible to reconstruct the field of a radiator in free space from the measurements of its field in a tank with reflecting boundaries. The approach under consideration allows the free-space calibration of the radiator in the tank avoiding the isolation of signals arriving at the receivers without boundary reflections. A key role in solving the inverse problem plays the tank calibration. This procedure gives the necessary values of the tank Green function, which accounts for multiple reflections of sound waves from the boundaries.

To test the feasibility of the proposed approach, a tank experiment was carried out. Analysis of the experimental data confirmed our assumption that equivalent sources reproducing the field of the radiator in free space reproduce the field of the same radiator in the tank. It was also demonstrated that the proposed method allows one reconstructing the fields of an acoustic monopole, dipole, and quadrupole in free space by measuring the fields of these sources in the tank.

As noted earlier, the weak point of the method of equivalent sources and, accordingly, the weak point of our approach is the lack of general rules for choosing the necessary number of equivalent sources and their positions. In our case, this difficulty is reinforced by the requirement that the same sources provide a sufficiently accurate approximation of the radiator field by the sum (1) in free space and by the sum (7) in the tank. In section 2.2 conditions (i) - (iv) are listed, which we consider necessary for this. However, these conditions are formulated in too general terms and they need to be made more precise and concrete.

Finally, it should be noted that the equivalent source method is used to analyze the scattered fields [7, 9]. The approach considered in this paper can also be applied for this purpose. With it, one can reconstruct the field scattered on the body in free space from the measurements of the field scattered on the same body in the tank. To solve this problem, the scatterer together with the radiator can be considered as one single sound source. Then its field in free space can be reconstructed using the discussed approach.

Acknowledgements

The research was carried out within the state assignment of IAP RAS (Project #00035-2014-0011). We are grateful to Dr. L.Ya. Lyubavin for valuable discussions.

References

- [1] R.J. Bobber. *Underwater electroacoustic measurement*. CA: Peninsula Press, Los Altos, 1988.
- [2] S.P. Robinson. Review of methods for low frequency transducer calibration in reverberant tanks, 1999. NPL Report CMAM 034.
- [3] S.P. Robinson, G. Hayman, P.M. Harris, and G.A. Beamiss. Signal-modelling methods applied to the free-field calibration of hydrophones and projectors in laboratory test tanks. *Meas. Sci. Technol.*, 29:085001, 2018.
- [4] A.E. Isaev and A.N. Matveev. Calibration of hydrophones in a field with continuous radiation in a reverberating pool. *Acoust. Phys.*, 55(2):762–770, 2009.
- [5] G.H. Koopmann, L. Song, and J.B. Fahnlne. A method for computing acoustic fields based on the principle of wave superposition. *J. Acoust. Soc. Am.*, 86(6):2433–2438, 1989.
- [6] Y.I. Bobrovnikskii and T.M. Tomilina. General properties and fundamental errors of the method of equivalent sources. *Acoustical Physics*, 41:649–660, 1995.
- [7] M.E. Johnson, S.J. Elliott, K-H. Baek, and J. Garcia-Bonito. An equivalent source technique for calculating the sound field inside an enclosure containing scattering objects. *J. Acoust. Soc. Am.*, 104(3):1221–1231, 1998.
- [8] Y.-B. Zhang, F. Jacobsen, C.-X. Bi, and X.-Z. Chen. Near field acoustic holography based on the equivalent source method and pressure-velocity transducers. *J. Acoust. Soc. Am.*, 126(3):1257–1263, 2009.
- [9] Y.J.R. Gounot and R.E. Musafir. Simulation of scattered fields: some guidelines for the equivalent source method. *J. Sound Vibr.*, 330(15):3698–3709, 2011.
- [10] S. Lee. Review: the use of equivalent source method in computational acoustics. *Journal of Computational Acoustics*, 25(1):1630001, 2017.

- [11] E. Fernandez-Grande, A. Xenaki, and P. Gerstoft. A sparse equivalent source method for near-field acoustic holography. *J. Acoust. Soc. Am.*, 141(1):532–542, 2017.
- [12] T. Semenova and S.F. Wu. On the choice of expansion functions in the Helmholtz equation least-squares method. *J. Acoust. Soc. Am.*, 117(2):701–710, 2005.
- [13] G. H. Golub and C.F. Van Loan. *Matrix computations*. The John Hopkins University Press, Baltimore, 1989.
- [14] S. Gurbatov, M. Deryabin, V. Kurin, and D. Kasyanov. Evolution of intense narrowband noise beams. *J. Sound Vib.*, 439:208–218, 2019.